

Use of the subsurface thermal regime as a groundwater-flow tracer in the semi-arid western Nile Delta, Egypt

Zenhom E. Salem¹ · Dina A. Bayumy²

Received: 31 July 2014 / Accepted: 31 January 2016 / Published online: 19 February 2016
© Springer-Verlag Berlin Heidelberg 2016

Abstract Temperature profiles from 25 boreholes were used to understand the spatial and vertical groundwater flow systems in the Western Nile Delta region of Egypt, as a case study of a semi-arid region. The study area is located between the Nile River and Wadi El Natrun. The recharge areas, which are located in the northeastern and the northwestern parts of the study area, have low subsurface temperatures. The discharge areas, which are located in the western (Wadi El Natrun) and southern (Moghra aquifer) parts of the study area, have higher subsurface temperatures. In the deeper zones, the effects of faults and the recharge area in the northeastern direction disappear at 80 m below sea level. For that depth, one main recharge and one main discharge area are recognized. The recharge area is located to the north in the Quaternary aquifer, and the discharge area is located to the south in the Miocene aquifer. Two-dimensional groundwater-flow and heat-transport models reveal that the sealing faults are the major factor disturbing the regional subsurface thermal regime in the study area. Besides the main recharge and discharge areas, the low permeability of the faults creates local discharge areas in its up-throw side and local recharge areas in its down-throw side. The estimated average linear groundwater velocity in the recharge area is 0.9 mm/day to the eastern direction and 14 mm/day to the northwest. The average linear groundwater discharge velocities range from 0.4 to 0.9 mm/day in the southern part.

Keywords Egypt · Arid regions · Groundwater recharge/water budget · Groundwater flow · Thermal regime

Introduction

About 30 % of land area on the Earth is arid or semi-arid where potential evapotranspiration exceeds rainfall (McKnight and Hess 2000). These areas, collectively called ‘the arid and/or semi-arid zone’, constitute much of the Earth’s land between latitudes 18 and 40° north and south of the equator and include most of northern and southern Africa, the Middle East, western USA and the southern areas of South America, most of Australia, large parts of central Asia, and even parts of Europe (NOAA 2010). In these environments, low rainfall leads to correspondingly low and intermittent surface runoff, and groundwater is often the only reliable water resource. Ensuring sustainability of water resources in such areas requires a quantitative estimate of water-balance parameters such as recharge, discharge and rates of horizontal and vertical flow, as well as water residence time. In such regions, the net water flux to groundwater (defined as recharge) is generally a very small component of the total water balance and conventional approaches to estimate recharge are fraught with large uncertainties. Naturally occurring isotopic and chemical tracers were used to estimate recharge, discharge, and flow rates for arid-zone groundwater and were adopted soon after development of high-precision mass spectrometric and radiometric counting techniques (Aggarwal et al. 2005a). In this work, the authors used the subsurface thermal regime to understand the groundwater recharge, discharge and vertical flow rates in the western Nile Delta as a desert newly developed for agricultural purposes.

It has long been known that temperature can be an important tool for investigating groundwater flow. Bredehoeft and Papadopoulos (1965) published the first quantitative analysis of

✉ Zenhom E. Salem
zenhomsalem@yahoo.com

¹ Geology Department, Faculty of Science, Tanta University, Tanta 31527, Egypt

² Ministry of Irrigation and Water Resources, Giza, Egypt

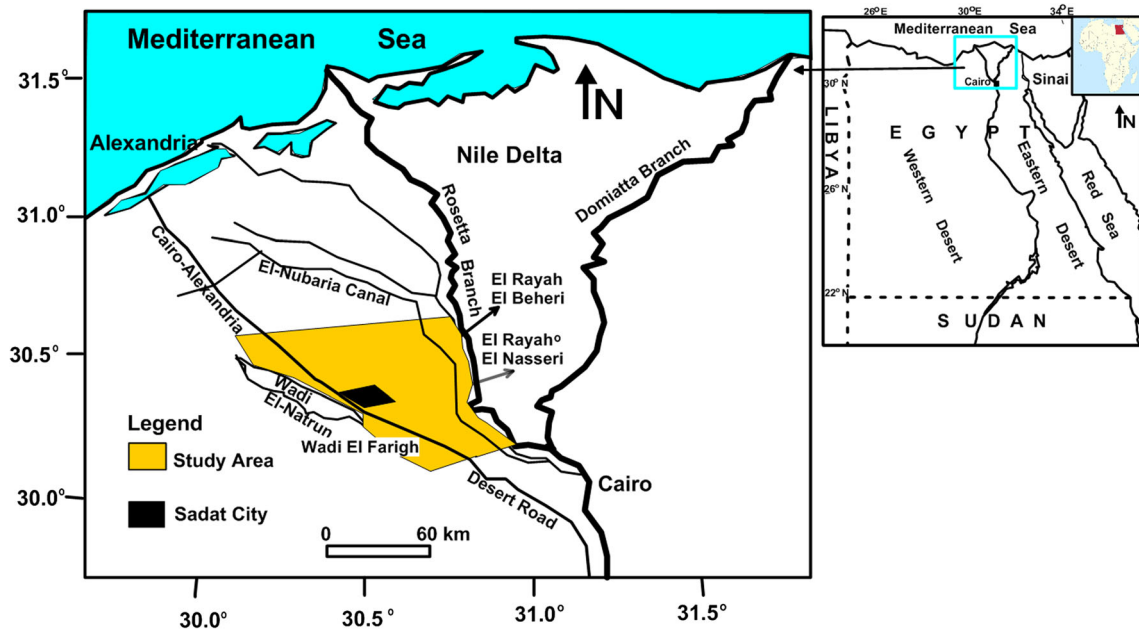


Fig. 1 Location map of the study area

the steady, one-dimensional (1D) transport of heat by groundwater flow through a semi-confined aquifer, although they

cited conceptual works on the subject written as early as 1934. They showed how a vertical temperature profile could

Fig. 2 Map showing the spatial distribution of the four aquifers in the study area (after Embaby 2003) superimposed by the estimated geologic structures

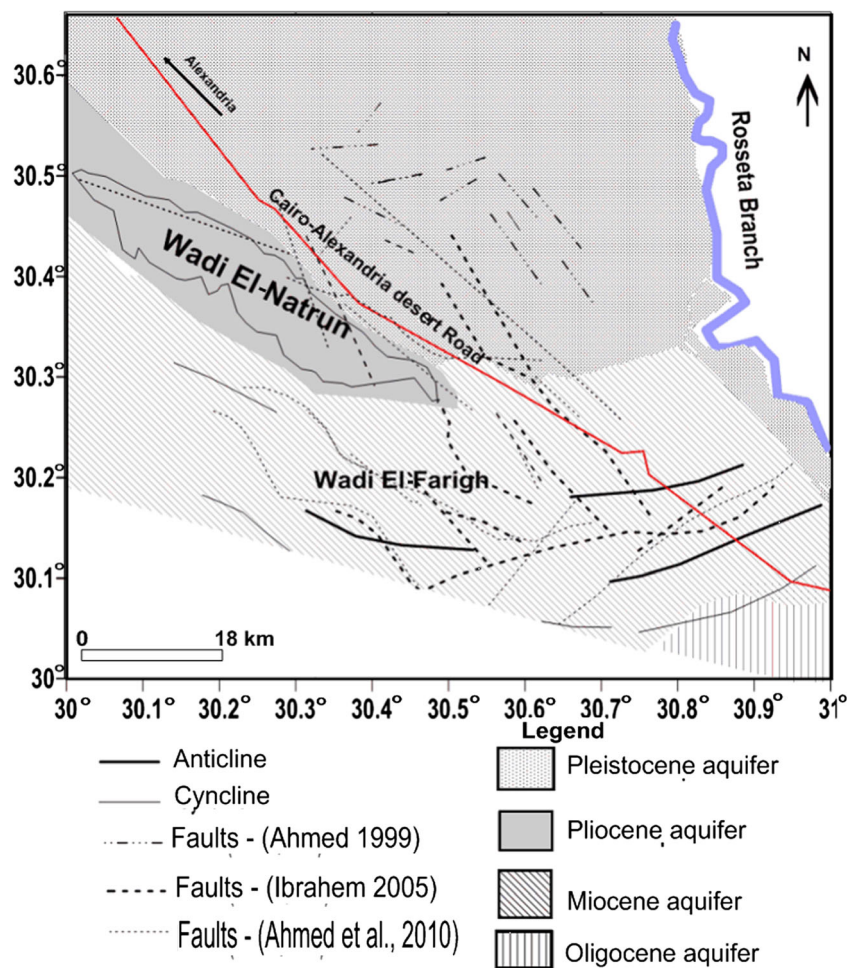
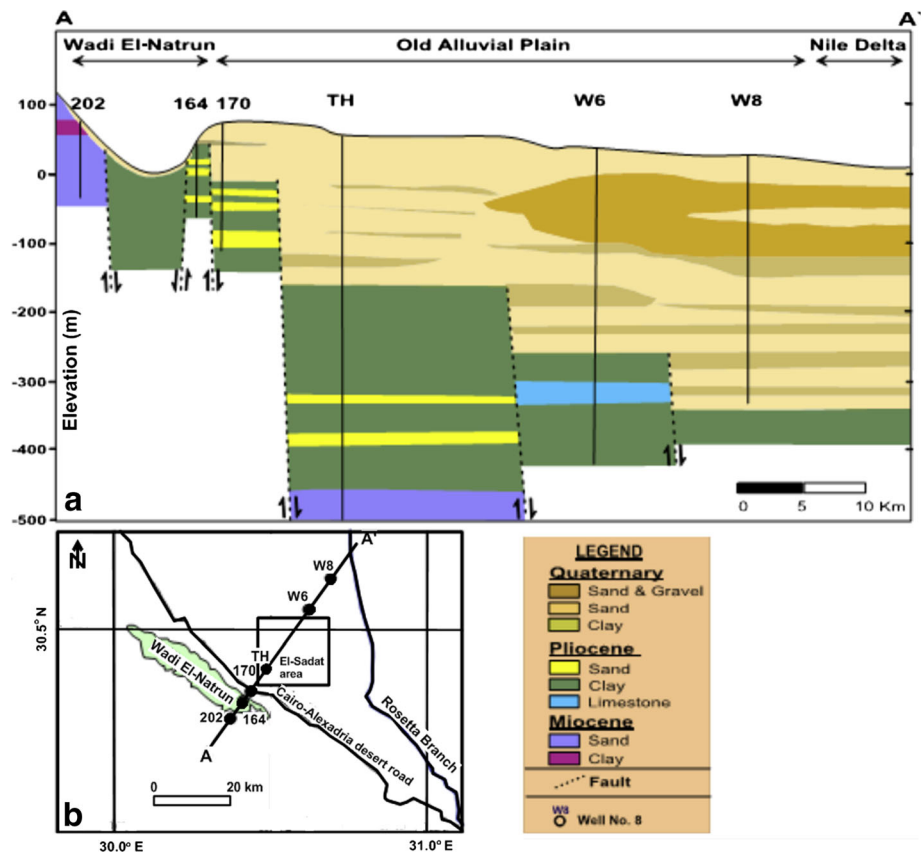


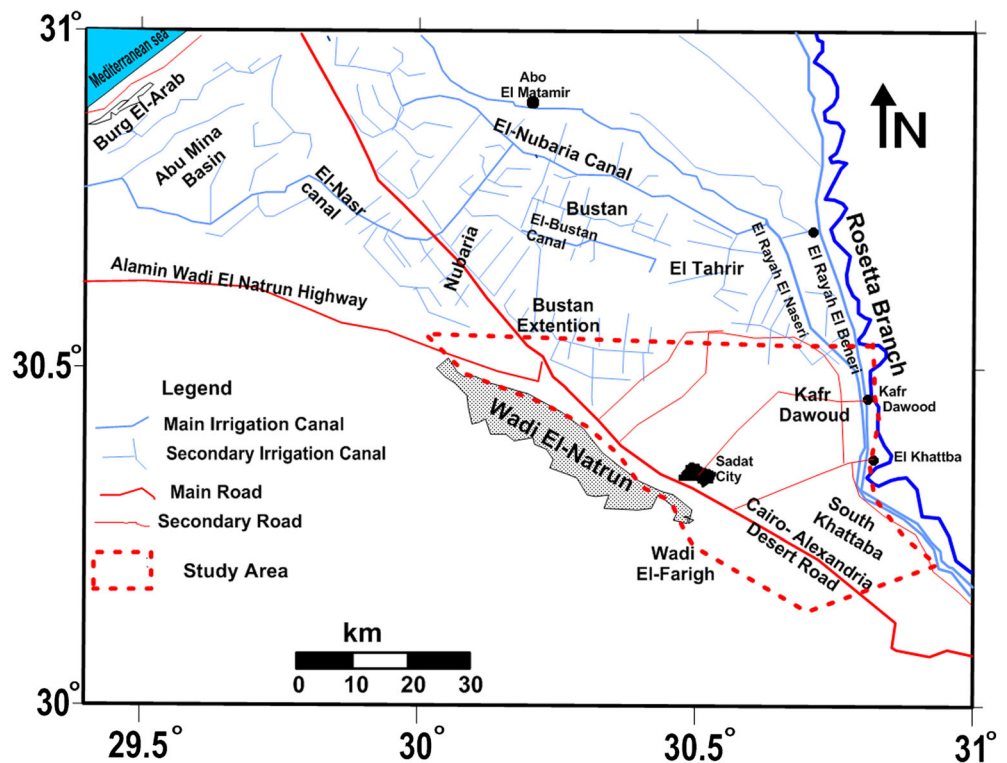
Fig. 3 Vertical 2D cross-section (a) and its location (b), illustrating the lithological composition of the Quaternary, Pliocene and Miocene aquifers and the structural contact between them (after El-Abd 2005 and Massoud et al. 2014)



be used to constrain the hydraulic properties of a postulated confining layer, and presented a set of type-curves to be

matched against field data for this purpose (Bredehoeft and Papadopulos 1965). A number of researchers have

Fig. 4 Surface-water system in the study area and its vicinities (after Embaby 2003)



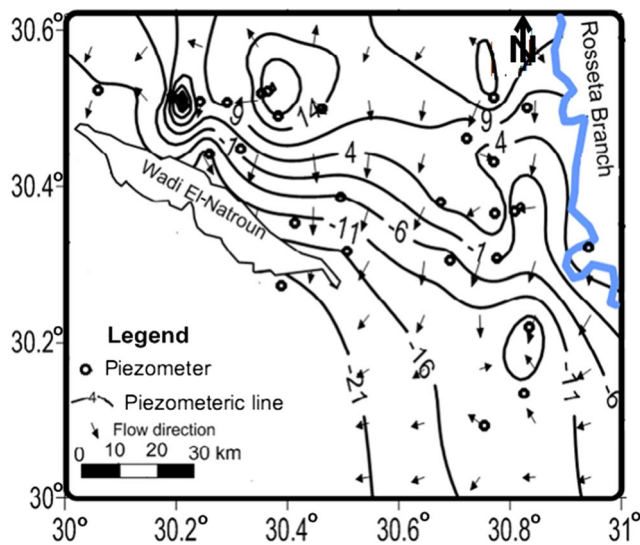


Fig. 5 The distribution of hydraulic head and the groundwater flow pattern in the study area (current study 2010)

investigated subsurface fluid flow using temperature measurements in wells (Lachenbruch and Sass 1977; Sakura 1978; Bodvarsson et al. 1982, 2003; Sass and Lachenbruch 1982; Sass et al. 1988; Inagaki and Taniguchi 1994; Ge 1998; Sakura 1993; Lu and Ge 1996; Uchida et al. 1999; Deming 2002; Miyakoshi et al. 2003; Salem et al. 2004a, b; Majumder et al. 2013) and geothermal springs (Fairley et al. 2003; Fairley and Hinds 2004), or by remote sensing of ground temperatures (Coolbaugh et al. 2003). Many other research works are cited in Anderson (2005) and Saar (2011).

The groundwater temperature measured in observation wells is assumed to be the same as the rock matrix temperature (Taniguchi et al. 1999), because groundwater and enclosing rock matrix are likely to be in equilibrium. Temperature-depth profiles can be used to estimate the subsurface water fluxes. A temperature-depth profile in the absence of vigorous groundwater flow generally has a constant linear gradient governed by heat conduction. Domenico and Palciauskas (1973) analyzed the two-dimensional (2D) groundwater temperature distribution in a regional groundwater flow system and found that the temperature-depth profile shows a convex-downward shape in the recharge area where groundwater flow is predominantly downward and a convex-upward shape in the discharge area where groundwater flow is predominantly upward. If hot water originating from depth invades an aquifer through faults or fracture zones, temperature will decrease along the flow direction, creating positive geothermal anomaly centers around the invasion zone.

In the Nile Delta and Wadi El Assiuty in Egypt, Salem (2009a, b) used subsurface temperature, hydraulic heads and hydrochemistry as a multi-tracing method to delineate groundwater flow and its interaction with the nearby surface water. Subsurface temperature has also been used in the Nile Delta to map the groundwater flow and seawater invasion (Salem et al. 2008). In the present study, borehole temperature measurements were employed to constrain groundwater flow in a study area located between the Nile River (Rosseta branch) and the Wadi El Natroun in the western Nile Delta, Egypt (Fig. 1).

Fig. 6 Map showing the locations of the used boreholes and the 2D vertical cross-sections

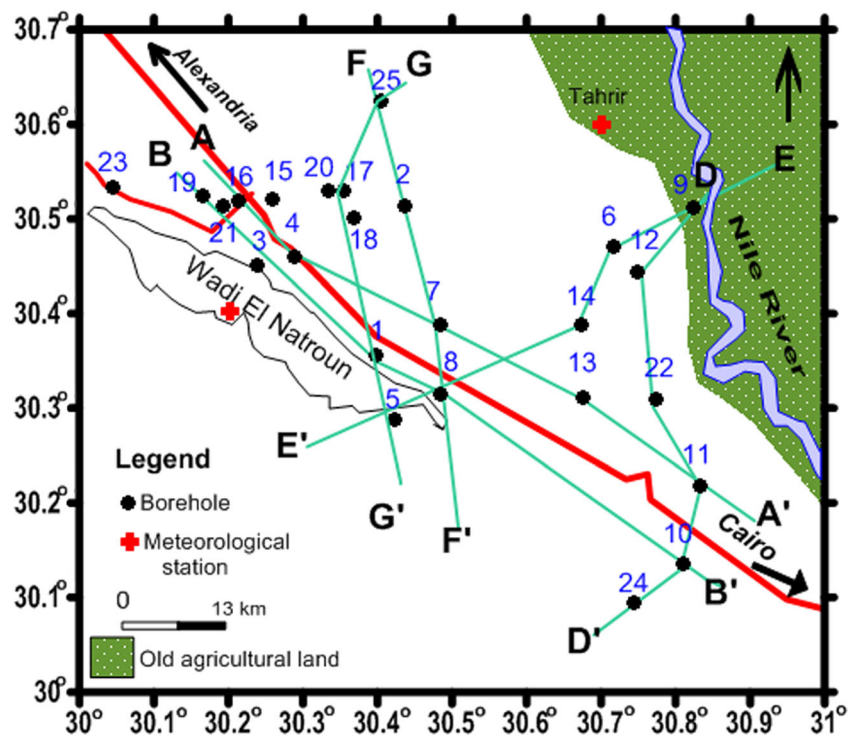
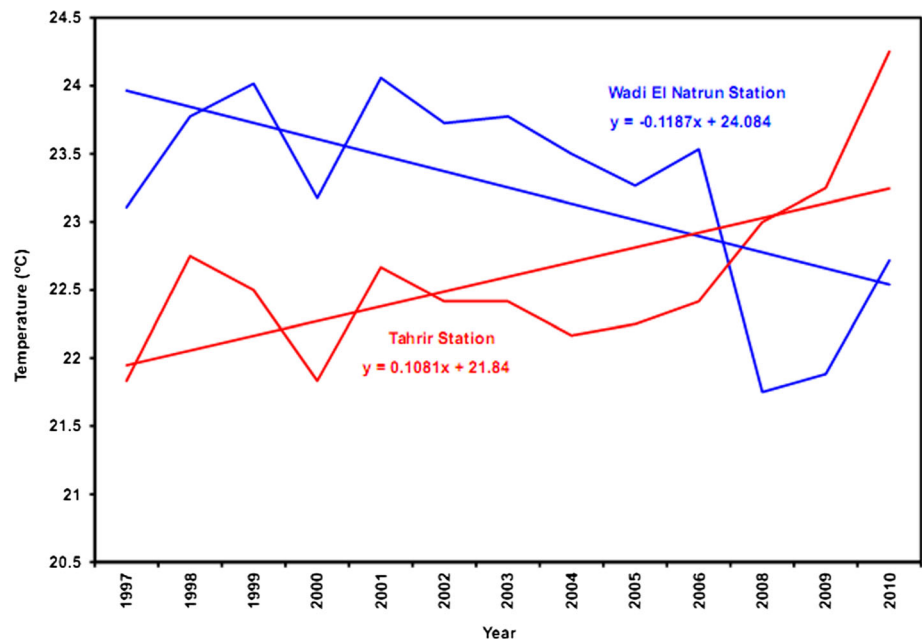


Fig. 7 Change in the mean annual surface air temperature during 1997–2010 for Tahrir (red) and Wadi El Natrun stations (blue). Tahrir station shows warming trend, while Wadi El Natrun station has a cooling trend



Study area

Over the last 50 years, several land development activities have been undertaken in the western Nile Delta region that affect both surface water and groundwater. Development of the Egyptian deserts, especially in the western Nile Delta, has become one of the main national interests. According to El-Gamal (2005), large reclamation projects, supplied with surface water from the River Nile, started in the 1960s. These projects have been implemented by the government and cover a total area of 252,000 ha. Since 1985, extensive land development activities have started based only on groundwater, mainly confined to the area south and east of Wadi El Natrun (total area amounts to 107,100 ha). This development is mainly handled by the private sector. As the reclamation processes affect groundwater quantities and flow, this study therefore aims to use subsurface temperatures to demonstrate their ability to trace groundwater flow in a semiarid region undergoing rapid economic development.

The study area lies in the southwestern Nile Delta, between the Rosetta Branch of the River Nile and the Wadi El Natrun, including Sadat City. It is bounded from south and north by latitudes 30.0 N and 30.6 N, respectively (Fig. 1).

Aquifer systems

The water-bearing formations in the investigated area are classified into four aquifers: the Quaternary, Pliocene, Miocene and Oligocene aquifers (Fig. 2). These aquifers are hydraulically connected and considered to be one hydrological unit. The Quaternary aquifer occupies the major part of the investigated area and it is essentially composed of fluvatile graded

sand and gravel intercalated with thin clay lenses (Fig. 3; El-Gamal 2005). The hydraulic conductivity of the Pleistocene aquifer ranges from a few meters per day to nearly 60 m/day (Gomaa 1995). Successive faults are controlling the relation between the Quaternary aquifer and the underlying Pliocene

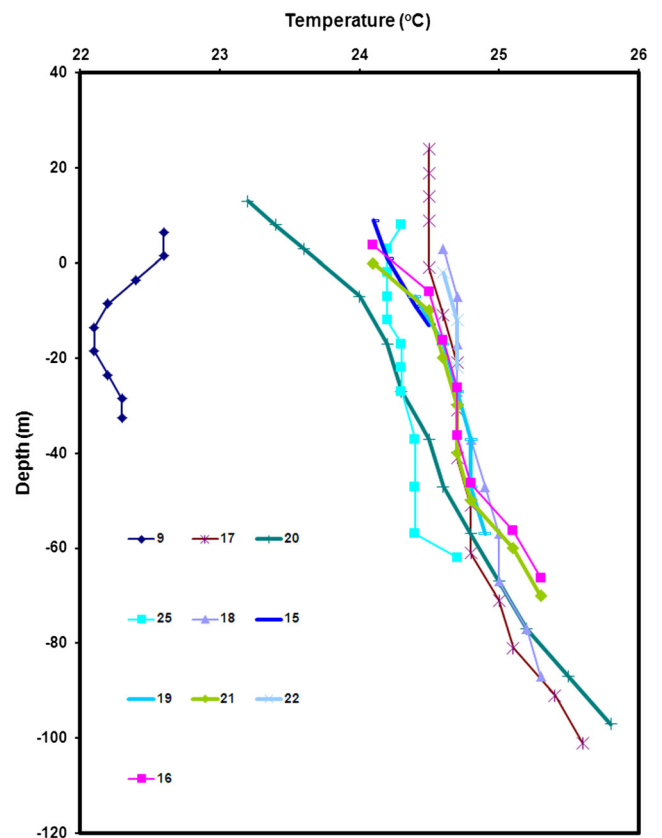


Fig. 8 Temperature-depth diagram of the encountered recharge type profiles

and Miocene aquifers. The Quaternary aquifer recharges mainly from the Nile water, infiltration of irrigation water and from the adjacent canals. Discharge from this aquifer occurs either naturally or artificially. Natural discharge occurs mainly through other aquifers. The artificial discharge occurs through hundreds of production wells.

The Pliocene aquifer is mainly restricted to the Wadi El Natrun depression; its sediments are composed of clay facies with interbeds of water-bearing sandy layers (Fig. 3). The thickness of the aquifer deposits is about 140 m at Wadi El Natrun, with a saturated thickness of about 90 m. The hydraulic conductivity of the Pliocene aquifer is about 10 m/day (Gomaa 1995).

The Miocene sediments are represented by the Moghra Formation, and are mainly composed of sand, sandstone and clay interbeds with vertebrate remains and silicified wood (Said 1962; Fig. 3). These sediments are occasionally overlain by Quaternary deposits and are underlain by the Oligocene basaltic sheet. The total thickness of the Miocene sediments reaches about 250 m at Wadi El Natrun. Regionally this thickness increases toward the northwest (El Ghazawi and Atwa 1994). The faults that are found in the area (Fig. 2) are responsible for elevating the Oligocene basaltic sheet and the underlying clay beds in the northeastern side (El Ghazawi and Atwa 1994).

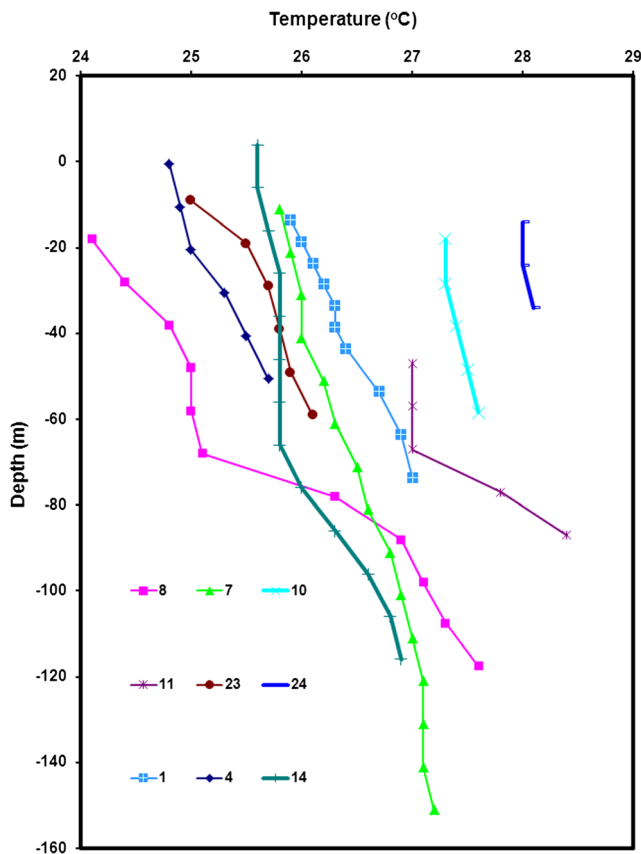


Fig. 9 Temperature-depth diagram of the encountered discharge type profiles

Surface-water system

The surface-water system includes the Rossetta branch of the Nile River and El Rayah El Beheri, El Rayah El Naseri, El Naburiya, El Naser and El-Bustan canals (Figs. 1 and 4). A large network of secondary channels was constructed in the western Nile Delta for irrigation purposes. These canals play an important role in the groundwater regime of the study area. The existing surface-water systems mainly cut through sand; therefore, there is a direct seepage from the surface water to groundwater.

Groundwater movement

The constructed piezometric map (Fig. 5) reveals the following: (1) groundwater movement is from the east and north directions where the surface-water sources are located (Fig. 4) toward the west and south directions; (2) Wadi El Natrun acts as a natural discharge area for the groundwater; and (3) the hydraulic gradient increases gradually from east to west with a marked increase close to Wadi El Natrun that is related to a natural discharging effect and to the presence of fault lines (Figs. 2 and 3) around both the eastern and northern sides of Wadi El-Natrun depression (Abdel Baki 1983). The fault effect and differences in the hydraulic conductivity

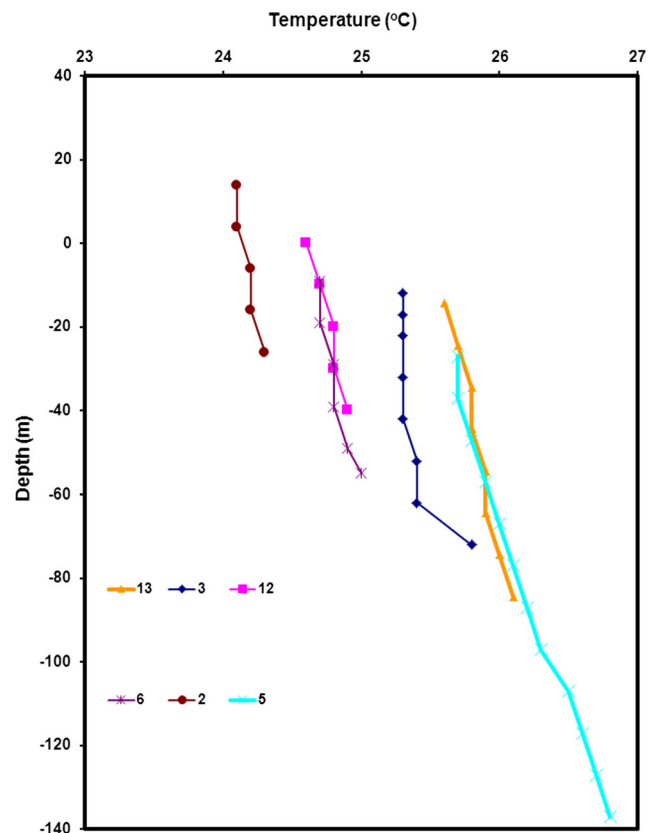


Fig. 10 Temperature-depth diagram of the encountered intermediate type profiles

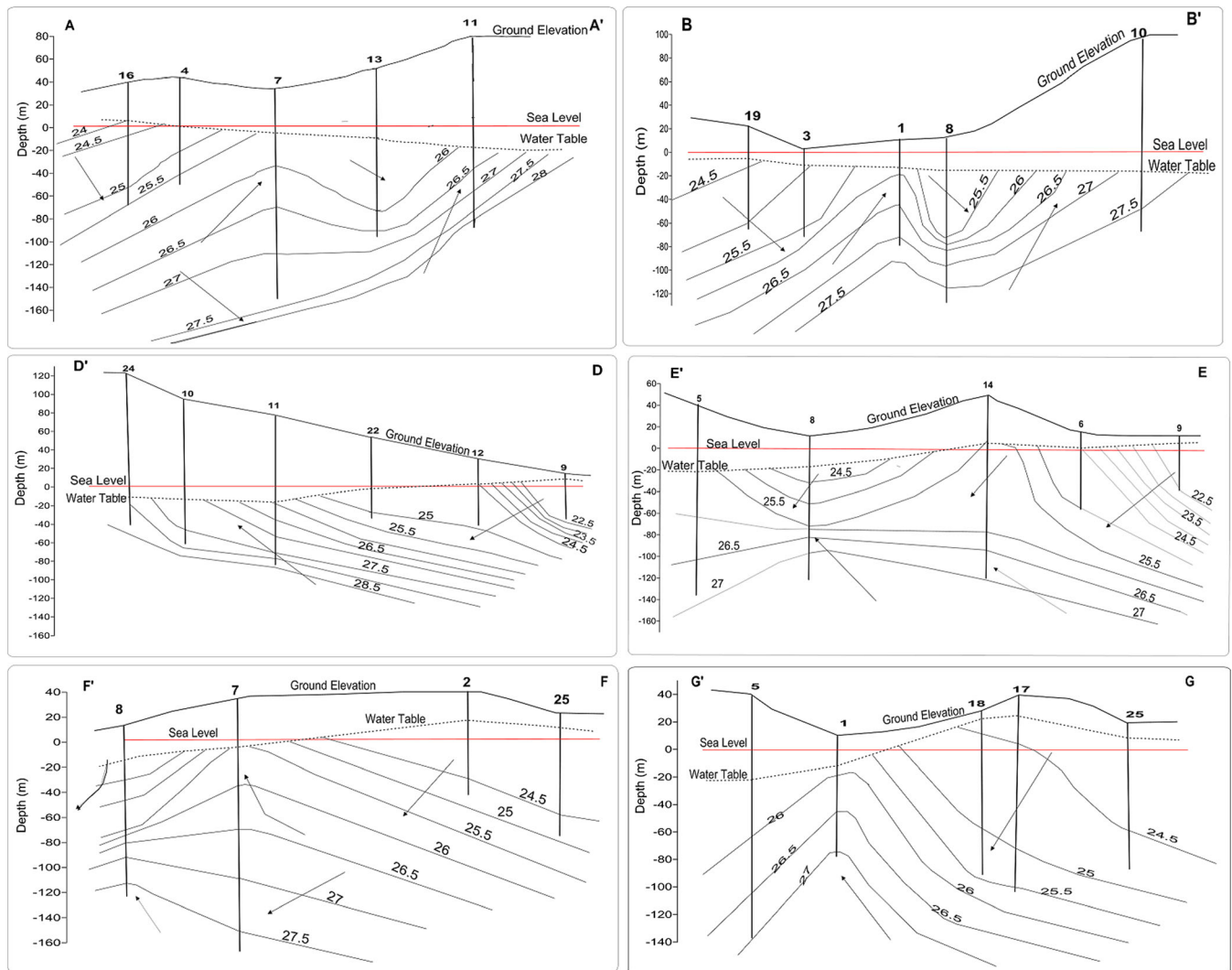


Fig. 11 Six vertical 2D cross-sections illustrating the relation between the subsurface temperature distribution and groundwater flow system and faults effects. *Arrows* indicate the estimated groundwater flow direction

between the three aquifers might play an important role in the groundwater flow regime, as will be shown in the next sections.

Methodology

Temperature-depth profiles were measured in 25 observation wells (up to 200 m depth; Fig 6). The equipment used for the measurements is a digital thermistor thermometer (resolution of 0.1 °C). Data were recorded from the water table to the bottom of the hole. According to Sorey (1971), free convection occurs in large-diameter boreholes cased with steel, which has higher thermal conductivity. However no free convection occurs in small-diameter boreholes cased with plastic materials, which have low thermal conductivity; therefore, free convection is not expected in the used boreholes because they were cased by plastic pipes mostly with a small average

diameter of 20 cm. The logged boreholes were cased and drilled at least 4 years before temperature logging in 2010; thus, the water temperatures in the boreholes represent the real formation temperatures.

Results and discussion

Surface air temperature

Figure 7 shows the change in the mean annual air temperature at Tahrir station located in the old agricultural land, and Wadi El Natrun station located in the newly developed land (for location see Fig. 6). The air temperatures of the last 14 years show a warming trend in Tahrir and a cooling trend in Wadi El Natrun. The Tahrir trend follows the general trend of global and local warming, whereas the cooling trend in Wadi El Natrun area could be related to the agricultural development

processes, as this is the main environmental change that has happened during the last few decades. Due to the lack of enough past temperature data, the noticed warming and cooling trends are not the result of just 14 years but may be related to several decades.

One-dimensional subsurface temperature profiles

Field temperature data are represented in Figs. 8, 9, and 10. The borehole temperatures vary from 22 to 28.4 °C in well 9 close to the Nile River and well 24 at the southern part of the area, respectively. For detailed study, the profiles are classified into three groups according to the well location (see Fig. 5).

Although the shapes of the curves in Figs. 8, 9, and 10 are similar, temperatures in Fig. 8 (wells 9, 15, 16, 17, 18, 19, 21, 22 and 25) tend to be lower overall than in Fig. 9 (wells 1, 4, 7, 8, 10, 11, 14, 23, and 24). This is because Fig. 8 profiles fit with the recharge area, while Fig. 9 profiles fit with the discharge area. The recharge processes affect the thermal profiles of the first group (Fig. 8) due to either water seepage from Nile River (well 9) or surface infiltration as a result of irrigation processes (as in the other wells). The profile for well 9 has low temperatures compared to the other wells because it is located in the old agricultural land which has lower mean annual surface air temperature (21.9 °C) as shown at Tahrir station (Fig. 7). All the other wells of this study are located in the developed land, which has higher surface air temperature (24 °C) as shown at Wadi El Natrun station (Fig. 7). Groundwater discharge processes affecting the temperature profiles of the second group (Fig. 9) occur in this area either by natural hydraulic conditions or through faults. The fault effect on the temperature profiles is clearly shown in boreholes 1, 7, 8 and 11. The third group of wells (2, 3, 5, 6, 12 and 13; Fig. 10) represents intermediate temperatures and are mostly located in the intermediate area between the recharge and the discharge areas.

Vertical 2D subsurface temperature distribution

Six vertical 2D cross-sections (Fig. 11) were constructed in the direction of groundwater flow to explain the subsurface temperature distribution in relation to the groundwater flow system, and pass through the areas of expected structures to show the fault effect. Subsurface temperature distribution along AA' cross section, which is located parallel and to the east of the Cairo–Alexandria desert road, is shown in Fig. 11. According to the net flow map (Fig. 5), the recharge area to the northwest is characterized by colder temperature compared to the discharge area in the southern part. Well 7 might be affected by fault structure leading to formation of a local warm temperature zone due to local groundwater discharge. Cross-section BB' (Fig. 11) shows a similar vertical temperature distribution system to AA' with local upward groundwater at well 1 which might also be related to fault structure.

The northeast–southwest vertical 2D temperature distribution, from the area close to the Rosetta branch to the Moghra Formation (south of Wadi El Natrun), is shown in cross section DD' (Fig. 11). At the same levels, the southern area has higher temperatures compared to the northeastern part; therefore, the groundwater main recharge area is toward the northeast (well 9), and the discharge is due southwest (well 24). Cross section EE' (Fig. 11) shows 2D vertical distribution of the subsurface temperatures from the east where Nile River exists to Wadi El Natrun in the western direction. The main recharge area is located to the east and is characterized by low values of the isothermal lines. The main discharge area has higher values of the isotherms where well 5 is located. Local recharge areas with shallower effect are observed at well 14. The latter recharge areas were created due to extensive irrigation using groundwater which has warmer temperature compared with the average annual air temperatures.

The north–south vertical 2D subsurface temperature distribution along FF' and GG' show clearly the fault effect on the groundwater flow in the areas of wells 7 and 1, where a warm zone exists due to upward groundwater flow along the sealing fault zone. In the latter cross-sections, the warmer zone is followed by a low-temperature zone in the shallower depths, which

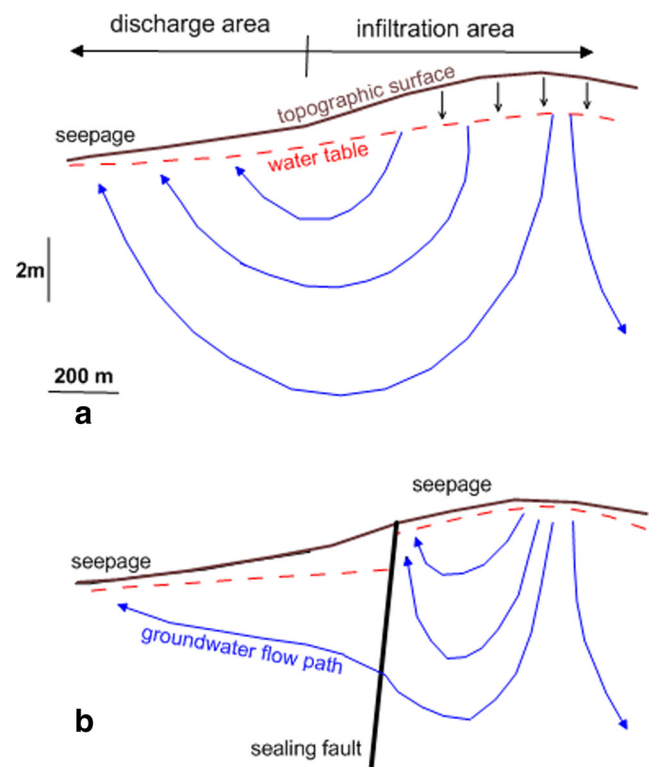


Fig. 12 Effect of low conductivity fault zone on the groundwater flow system (from Bense et al. 2003). **a** The groundwater flows from the recharge area to the discharge area without barriers. **b** The sealing fault controls the groundwater flow in the shallow zone where the groundwater flows upward in the right side. The fault also lowers the water level in the left side forming a shallow local recharge area. Arrows and the dashed lines indicate the groundwater flow and water table, respectively

could be related to the effect of the down-throw of the fault where the groundwater level became deeper to collect the waters from the surroundings (Bense et al. 2008) as shown in Fig. 12. In FF' and GG' cross sections, the main recharge area is located to the north where wells 2 and 17 exist and the discharge area is located to the south where wells 8 and 5 are located.

Horizontal 2D subsurface temperature distribution

Figure 13 represents the horizontal 2D subsurface temperature distribution at 20, 40, 60 and 80 m below sea level (bsl). Comparing temperatures of these levels (Fig. 13a,b,c,d) indicates that temperature values increase downward. Two main recharge areas are recognized where the isothermal lines have lower temperature values. The first area is located to the east and northeast, close to the Nile River where well 9 exists. The second area is noticed toward the northern direction of Wadi El Natroun. Seepage from the Nile River and the main channels located to the east and the northeast is the source of the recharge water in the first area, while irrigation canals and reclamation processes are the sources of the groundwater in the second area

(see Fig. 4). Two main discharge areas were also recognised with Wadi El Natroun being the first one, and has warmer isotherms compared to the northern and eastern portions. The area of wells 10 and 11 is considered a discharge area because it has the highest temperature values. The fault effect is noticed in the areas of wells 1 and 7. Faults formed a local warm area at wells 1 and 7 because they force the groundwater to flow upward along the sealing fault zones. Faults have also formed a local recharge area with shallower effect on their down-throw side where well 8 exists. The observed impact of the fault located to the west and the recharge process in the northeastern direction on the temperature distribution completely disappear at 80 m depth, except for a minor temperature anomaly at well 7 (Fig. 13d). The area in the northwestern direction is the only recharge area recognized at that depth and the main discharge area is observed to the south where well 11 is located.

Numerical modeling

Among the constructed 2D cross-sections of the observed temperatures, three cross sections (AA', DD' and GG'; Fig. 11)

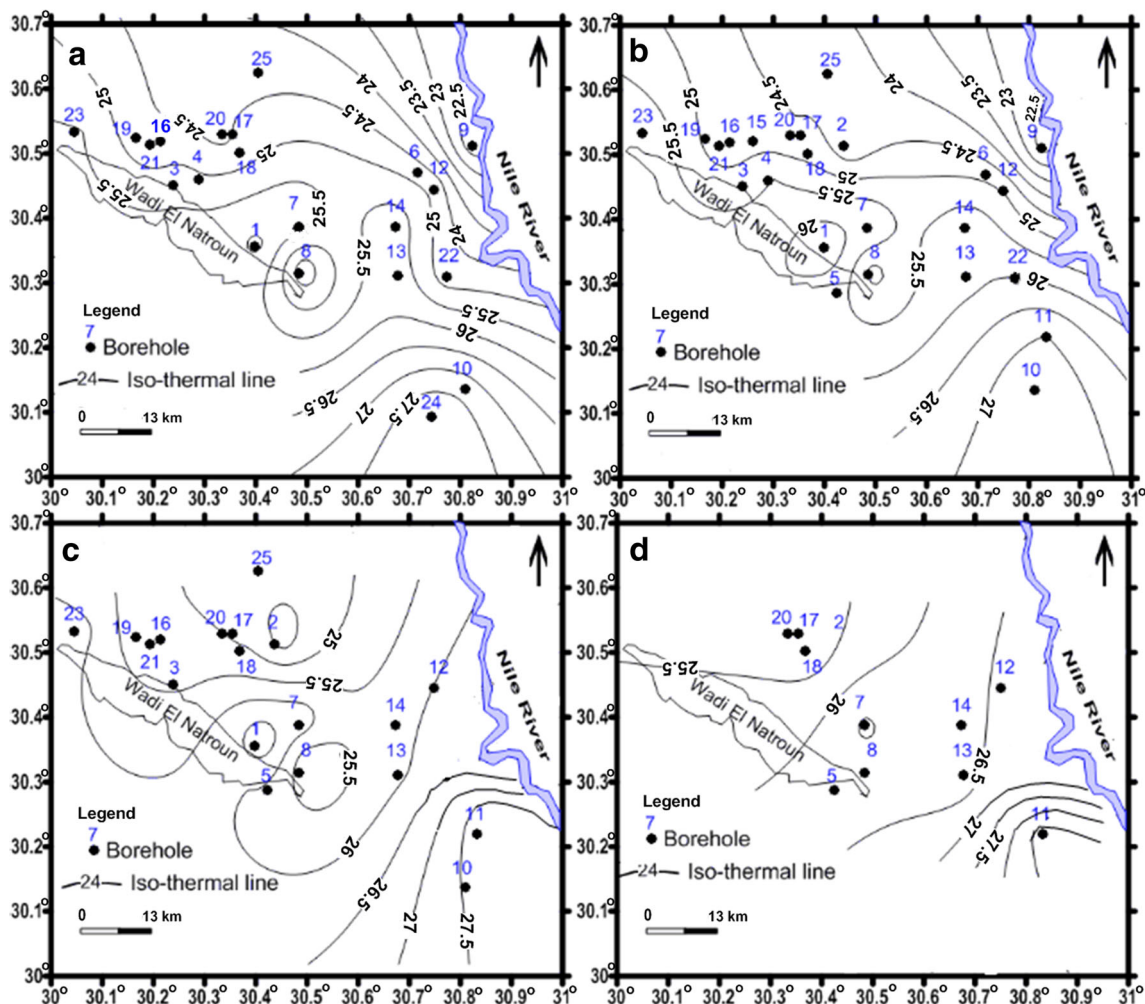
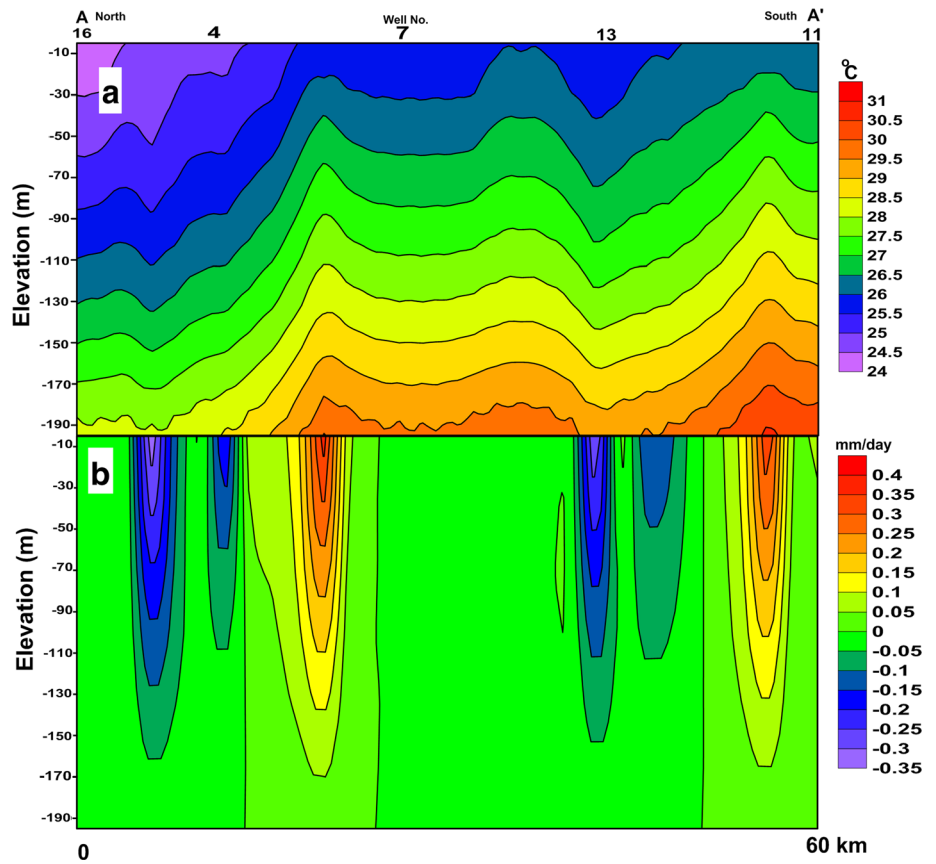


Fig. 13 Maps show the horizontal 2D spatial subsurface temperature distributions at 20, 40, 60 and 80 mbsl (a, b, c and d, respectively)

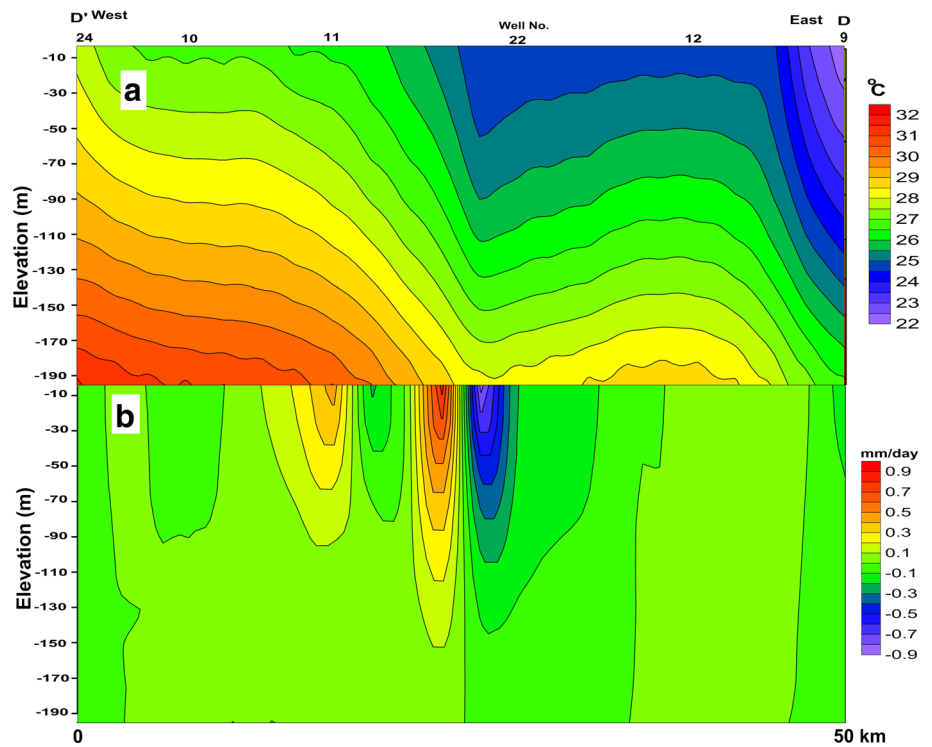
Fig. 14 Simulated **a** vertical 2D temperature distribution along the cross-section AA' and **b** the groundwater velocity along the same cross-section. The simulated thermal regime in **(a)** is similar to the observed temperatures represented in (Fig. 11). *Negative velocity values* indicate the recharge system, while the *positive values* represent the discharge system



were selected for simulation models. These cross-sections were chosen to illustrate the potential effects of thermal conduction

and advection transports along the groundwater flow system in three different directions and to show the fault effect. The

Fig. 15 Simulated **a** vertical 2D temperature distribution along the cross-section DD' and **b** the groundwater velocity along the same cross-section. The simulated thermal regime in **(a)** is similar to the observed temperatures represented in (Fig. 11). *Negative velocity values* indicate the recharge system, while the *positive values* represent the discharge system



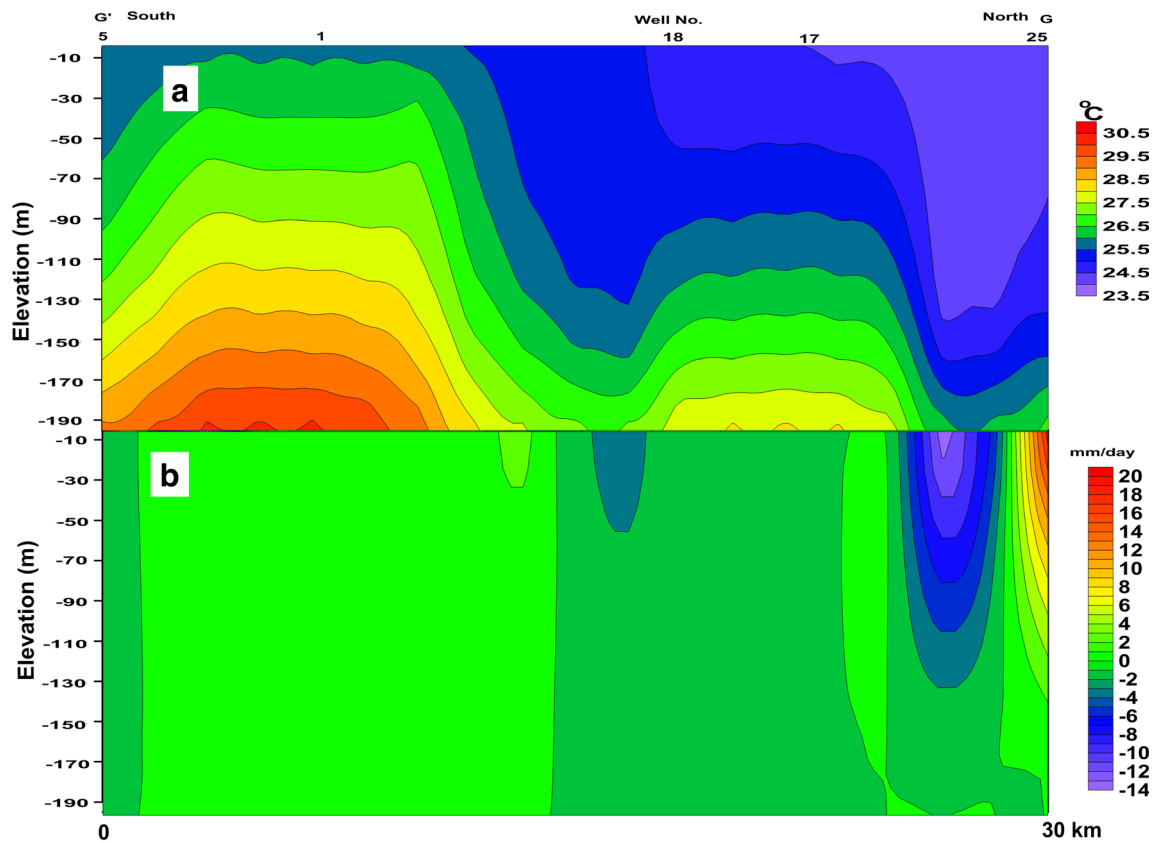


Fig. 16 Simulated **a** vertical 2D temperature distribution along the cross-section GG' and **b** the groundwater velocity along the same cross-section. The simulated thermal regime in (a) is similar to the observed

temperatures represented in (Fig. 11). *Negative velocity values* indicate the recharge system, while the *positive values* represent the discharge system

Simulator for HEat and MAss Transport (SHEMAT) was chosen to carry out the numerical simulations, because together with Processing SHEMAT (Kühn and Chiang 2004), it is an easy-to-use general-purpose reactive transport code for a wide variety of thermal and hydrogeological problems in two and three dimensions. SHEMAT solves coupled problems involving fluid flow, heat transfer, species transport, and chemical water–rock interaction in fluid saturated porous media on a Cartesian grid. In SHEMAT, the different flow, transport, and reaction processes can be selectively coupled. Flow and heat transport are coupled in the way that the fluid parameters density, viscosity, compressibility, thermal conductivity, and thermal capacity are functions of temperature and pressure. A detailed description of the governing equations and code verifications are given by Clauser (2003). The convective term of the heat-flow problem was approximated by the II' in-flux-blending scheme (Bartels et al. 2000). The measured hydraulic head and temperatures at the groundwater surface were used as the constant upper boundary. The depth of the three models started from sea level down to 200 m (20 rows, each 10 m thick). The length of the cross-sections depends on the horizontal extension of the models. The lengths for models AA', DD' and GG' (Figs. 14, 15, and 16) are 60, 52 and 30 km (500 m for each column).

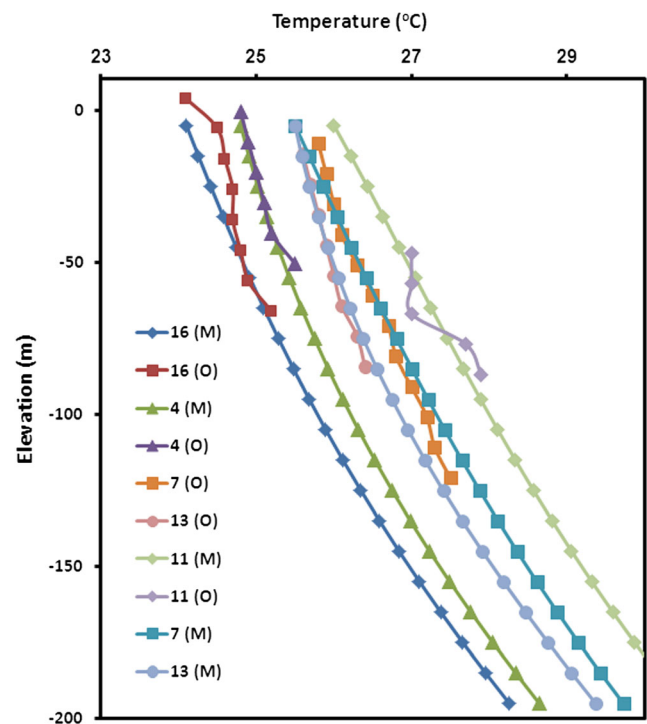


Fig. 17 A comparison between the observed (O) and modeled (M) temperature profiles of the cross-section AA' (Figs. 11 and 14a)

The used initial hydraulic heads were set according to the measured data. Measured temperatures at the water table were used as the initial temperatures. The basal heat-flow density was set constant at 0.08 W/m^2 (Kühn and Chiang 2004). Initial fluid pore-pressure conditions are defined to be hydrostatic. According to El-Bayomy (2015), the porosity and permeability are set with a variable range from 30 to 15 % and from 10^{-12} m to 10^{-14} m^2 , respectively. The eastern and the northwestern parts have 30 % porosity and 10^{-12} m^2 permeability; in contrast, the western and the southern parts have lower porosity and permeability, reaching 15 % and 10^{-14} m^2 , respectively. During the simulation process, the most sensitive parameter was permeability. The initial thermal matrix property parameters were set uniform for the entire model. $2.9 \text{ W/(m} \cdot \text{K)}$ and $800 \text{ J/(kg} \cdot \text{K)}$, were used respectively, for thermal conductivity and specific heat capacity. It is assumed that there are neither fluid heat sources nor radiogenic heat production within the model area.

The general groundwater thermal regime and velocity distributions in the three model domains can be seen in Figs. 14, 15, 16, 17, 18, and 19 show the fit between observed and simulated temperatures for each borehole in the three models. It is clearly shown that the isotherms are affected by the recharge, discharge and faults. Temperatures are lower in groundwater downward-flow areas (recharge) and higher in the upward flowing areas (discharge). The main recharge areas are noticed in Figs. 14a and 16a to the north and in

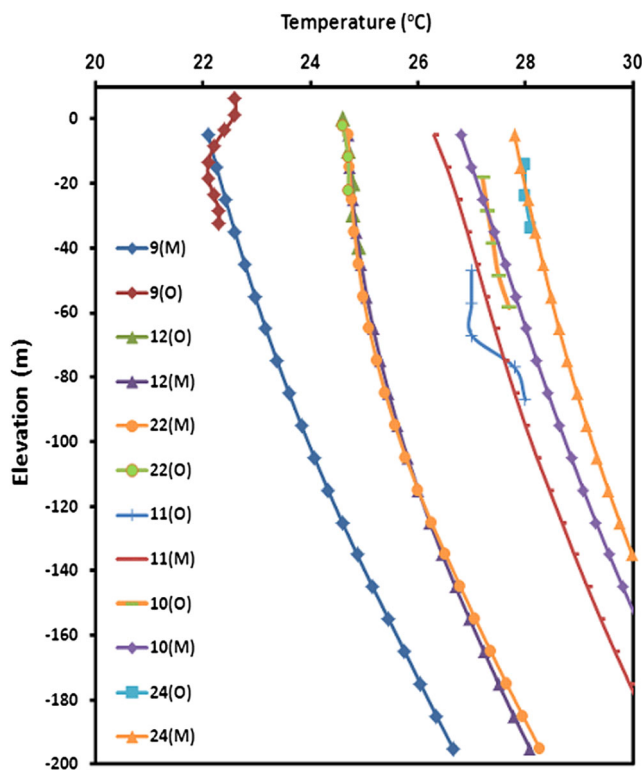


Fig. 18 A comparison between the observed (O) and modeled (M) temperature profiles of the cross-section DD' (Figs. 11 and 15a)

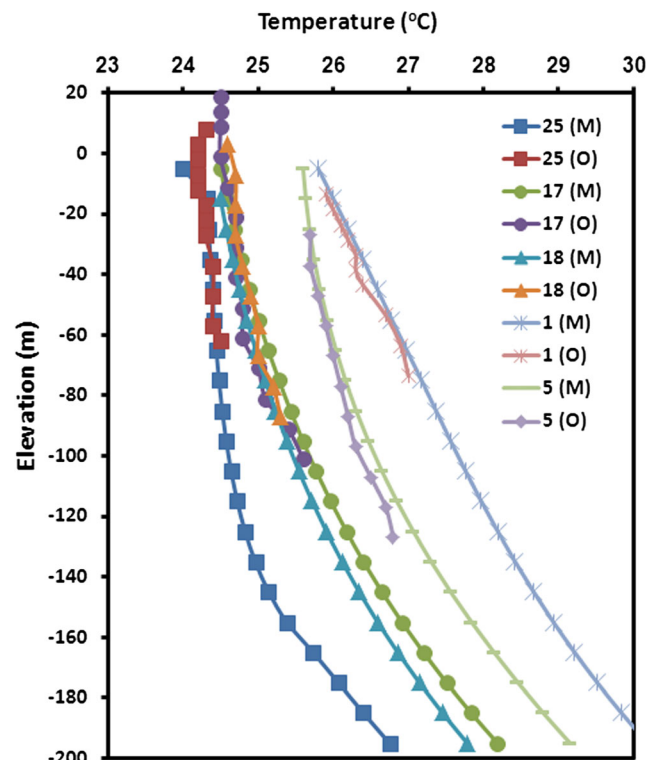


Fig. 19 A comparison between the observed (O) and modeled (M) temperature profiles of the cross-section GG' (Figs. 11 and 16a)

Fig. 16a to the east. The main discharge areas are noticed to the south in Fig. 14a and in Fig. 16a to the west. According to the lithological cross-section shown in Fig. 3, the area has a successive fault system raising the clay-rich Pliocene and Miocene deposits upward. These faults are affecting the temperature distribution by efficiently transporting thermal energy upwards forming local groundwater discharge areas in the low-permeability (10^{-14} m^2) up-throw side of the faults as shown in Figs. 14a (well 7), 15a (well 12) and 16a (wells 17 and 1). Accordingly, several local recharge areas characterized by a cooling effect, where the groundwater infiltrated downward, are encountered in the down-throw area of the faults (permeability ranges from 10^{-12} to 10^{-13} m^2). The latter phenomenon is clearly shown in the areas of well 13 (Fig. 14a) and well 22 (Fig. 15a), and the area located between wells 18 and 1 (Fig. 16a).

The groundwater in the three simulated cross-sections is actively circulating in the shallow zone but in the deep zones it mostly flows in a horizontal direction where the vertical speed nearly equals zero. The ranges of the vertical velocity of the recharged water in the three cross-sections are $0.0\text{--}0.35 \text{ mm/day}$ (Fig. 14b), $0.0\text{--}0.9$ (Fig. 15b) and $0\text{--}14 \text{ mm/day}$ (Fig. 16b). The latter values mean that the main recharge area of the study groundwater is mainly located to the northwestern direction. On the other hand, the ranges of the vertical discharge velocities of the groundwater are $0\text{--}4 \text{ mm/day}$ (Fig. 14b), $0\text{--}0.9 \text{ mm/day}$ (Fig. 15b) and $0\text{--}20 \text{ mm/day}$ (Fig. 16b).

Conclusions

The western Nile Delta is a typical example of a semi-arid area with development activities, and subsurface temperature in the study area was used as a groundwater flow tracer. Observed temperature–depth profiles are classified into three types depending on the shape of the profile, temperature magnitude, and thermal gradient. Recharge-type wells are mainly located in the Quaternary aquifer in the northeast and northwest where downward groundwater fluxes are expected due to seepage from the Nile River and irrigation channels. On the other hand, wells with discharge type are located in the western and southern parts where Pliocene and Miocene aquifers are located. The groundwater flow systems estimated from the observed subsurface temperature agree well with the systems evaluated from hydraulic potentials. It also clearly shows the spatial and vertical effects of faults and different recharge sources. Fault zones are considered as upward passageways for the deeper warm groundwater. Faults also form a local shallow recharge area in their down-throw direction that is characterized by lower values of the isothermal lines. Recharge processes close to the Nile River and fault effects on the groundwater flow and isothermal lines diminish downward. At 80 mbsl, only one main recharge area is recognized to the north of Wadi El Natrun and also one major discharge area is noticed in the Miocene aquifer in the southern part of the area.

The simulated 2D cross-sections reveal that the sealing faults are the major factor disturbing the regional subsurface thermal regime in the area. Beside the main recharge and discharge areas, faults create local discharge areas in their up-throw side due to low permeability, and local recharge areas in their down-throw side. The estimated groundwater flux in the recharge area is 0.9 mm/day to the eastern direction and 14 mm/day to the northwest. The groundwater discharge velocities range from 0.4 to 0.9 mm/day in the southern part.

Acknowledgements The authors are grateful for Stephen Grasby and Martin Appold, associate editor and editor, respectively, of *Hydrogeology Journal* for their constructive remarks. Insightful reviews from Victor Bense and Grant Ferguson are greatly appreciated. The measured temperature data are taken from the master thesis of the second author; therefore, Abdel-Monem T. Abdel-Hameed and Taher M. Hassan are thanked for permitting the publishing of this work as they and the first author were supervising the thesis. This research was supported by funding from Tanta University, Egypt.

References

- Abdel Baki AA (1983) Hydrogeological and hydrogeochemical studies in the area west of Rosetta branch and south of El Nasr Canal. PhD Thesis, Ain Shams University, Egypt
- Aggarwal PK, Froehlich K, Gonfiantini R, Gat JR (2005) Isotope hydrology: a historical perspective from the IAEA. In: Aggarwal PK, Gat JR, Froehlich K (eds) *Isotopes in the water cycle: past, present and future of a developing science*. Springer, Berlin, 381 pp
- Bartels J, Kühn M, Pape H, Clauser C (2000) A new aquifer simulation tool for coupled flow, heat transfer, multi-species transport and chemical water rock interactions. Proceedings of World Geothermal Congress, Kyushu - Tohoku, Japan, May 28–June 10, 2000, pp 3997–4002
- Bense V, Person M, Chaudhary K, You Y, Cremer N, Simon S (2008) Thermal anomalies indicate preferential flow along faults in unconsolidated sedimentary aquifers. *Geophys Res Lett* 35:L24406. doi: [10.1029/2008GL036017](https://doi.org/10.1029/2008GL036017)
- Bodvarsson GS, Benson SM, Witherspoon PA (1982) Theory of the development of geothermal systems charged by vertical faults. *J Geophys Res* 87:9317–9328
- Bredehoeft JD, Papadopoulos IS (1965) Rates of vertical groundwater movement estimated from the Earth's thermal profile. *Water Resour Res* 1:325–328
- Clauser C (2003) SHEMAT and processing SHEMAT: numerical simulation of reactive flow in hot aquifers. Springer, Heidelberg, Germany
- Coolbaugh MF, Sawatzky DL, Oppliger GL, Minor TB, Raines GL, Shevenell LA, Blewitt G, Louie JN (2003) Geothermal GIS coverage of the Great Basin USA: defining regional controls and favorable exploration terrains. *Geotherm Resour Counc Trans* 27:9–13
- Deming D (2002) Introduction to hydrogeology. McGraw-Hill, New York
- Domenico PA, Palciauskas VV (1973) Theoretical analysis of forced convective heat transfer in regional groundwater flow. *Geol Soc Am Bull* 84:3803–3814
- El Ghazawi MM, Atwa SM (1994) Contributions of some structural elements to the groundwater conditions in the southwestern portion of the Nile Delta. *Geol Soc Egypt* 38:649–667
- El-Abd E (2005) The geological impact on the water bearing formations in the area south west Nile Delta, Egypt. PhD Thesis, Menoufia Univ., Egypt
- El-Bayomy DA (2015) Sedimentological and hydrogeological studies on the area west of the Nile Delta, Egypt. MSc Thesis, Tanta Univ., Egypt
- El-Gamal H (2005) Environmental tracers in groundwater as tools to study hydrological questions in arid regions. University of Heidelberg, Heidelberg, Germany
- Fairley JP, Hinds JJ (2004) Rapid transport pathways for geothermal fluids in an active Great Basin fault zone. *Geology* 32:825–828
- Fairley JP, Heffner J, Hinds JJ (2003) Geostatistical evaluation of permeability in an active fault zone. *Geophys Res Lett* 30:1962. doi: [10.1029/2003GL018064](https://doi.org/10.1029/2003GL018064)
- Ge S (1998) Estimation of groundwater velocity in localized fracture zones from well temperature profiles. *J Volcanol Geotherm Res* 84:93–101
- Gomaa MA (1995) Comparative hydrogeological and hydrogeochemical study on some aquifer west of Nile Delta, Egypt. PhD Thesis, Ain Shams University, Egypt
- Inagaki N, Taniguchi M (1994) Estimations of hydraulic conductivity and groundwater flow systems by using groundwater temperature in Nara Basin, Japan. *J Japan Assoc Hydrol Sci* 24:171–182
- Kühn M, Chiang HW (2004) Pre- and post-processing with “Processing SHEMAT”, in numerical simulation of reactive flow in hot aquifers: SHEMAT and processing SHEMAT. Springer, Heidelberg, Germany
- Lachenbruch AJ, Sass JH (1977) Heat flow in the United States and the thermal regime of the crust. In: Heacock JG (ed) *The earth's crust, its nature and physical properties*. American Geophysical Union, Washington, DC
- Lu N, Ge S (1996) Effect of horizontal heat and fluid flow on the vertical temperature distribution in a semiconfining layer. *Water Resour Res* 32:1449–1453

- Majumder RK, Shimada J, Taniguchi M (2013) Groundwater flow systems in the Bengal Delta, Bangladesh inferred from subsurface temperature readings. *J Sci Technol* 35:99–106
- Massoud U, Kenawy A, Ragab EA, Abbas MA, El-Kosery HM (2014) Characterization of the groundwater aquifers at El Sadat City by joint inversion of VES and TEM, NRIAG. *J Astronom Geophys*. doi:10.1016/j.nrjag.2014.10.001
- McKnight TL, Hess D (2000) Climate zones and types: dry climates (zone B), physical geography: a landscape appreciation. Prentice Hall, Upper Saddle River, NJ
- Miyakoshi A, Uchida Y, Sakura Y, Hayashi T (2003) Distribution of subsurface temperature in the Kanto Plain, Japan, estimation of regional groundwater flow system and surface warming. *Phys Chem Earth* 28:467–475
- NOAA (2010) JetStream: online school for weather. http://www.srh.noaa.gov/jetstream/global/climate_max.htm. January 2010
- Said R (1962) The geology of Egypt. Elsevier, Amsterdam
- Sakura Y (1978) Studies on groundwater circulation using temperature data. In: Kokon S (ed) Studies on water balance in Japan, Tokyo, 344 pp
- Sakura Y (1993) Groundwater flow estimated from temperatures in the Yonezawa Basin, northeast Japan. In: Tracers in hydrology. IAHS, Wallingford, UK, pp 161–170
- Salem ZE (2009a) Hydraulic head, subsurface temperature and water quality as reasons for deciphering the groundwater resources and flow pattern in Wadi El-Assuity, Egypt. *Sediment Egypt* 17:199–216
- Salem ZE (2009b) Natural and human impacts on the groundwater under an Egyptian village, central Nile Delta: a case study of Mehallet Menouf, 13th International Water Technology Conference (IWTC, 13), March 12–15, 2009. Hurghada, Egypt, 3:1397–1414
- Salem ZE, Sakura Y, Mohamed Aslam MA (2004a) The use of temperature, stable isotopes and water quality to determine the pattern and spatial extent of groundwater flow: Nagaoka area, Japan. *Hydrogeol J* 12:563–575
- Salem ZE, Taniguchi M, Sakura Y (2004b) Use of temperature profiles and stable isotopes to trace flow lines: Nagaoka Area, Japan. *Ground Water* 42:83–91
- Salem ZE, Gaame OM, Hassan TM (2008) Using temperature logs and hydrochemistry as indicators for seawater intrusion and flow lines of groundwater in Quaternary aquifer, Nile Delta, Egypt, 5th International Symposium on Geophysics (ISG 5). 27–29 Nov 2007, pp 25–38
- Sass JH, Lachenbruch AH, Dudley WW Jr, Priest SS, Munroe RJ (1988) Temperature, thermal conductivity and heat flow near Yucca Mountain, Nevada: some tectonic and hydrologic implications. *US Geol Surv Open File Rep* 87-649
- Taniguchi M, Shimada J, Tanaka T, Kayane I, Sakura Y, Shimano Y, Dapaah-Siakwan S, Kawashima S (1999) Disturbances of temperature-depth profiles due to surface climate-change and subsurface water flow: (1) an effect of linear increase in surface temperature caused by global warming and urbanization in the Tokyo metropolitan area, Japan. *Water Resour Res* 35:1507–1517
- Uchida Y, Sakura Y, Anderson MP (1999) Subsurface temperature field in the Nobi Plain, central Japan. In: Sakura Y, Tang C (eds) Proceedings of the International Symposium on Groundwater in Environmental Problems, Chiba University, Chiba, Japan, pp 43–46